Biochimica et Biophysica Acta 1798 (2010) 526–535

Contents lists available at ScienceDirect

Biochimica et Biophysica Acta

journal homepage: www.elsevier.com/locate/bbamem

Multimeric forms of the small multidrug resistance protein EmrE in anionic detergent

Denice C. Bay [a], R. Arief Budiman [b], Mu-Ping Nieh [c], Raymond J. Turner [a,*]

[a] Department of Biological Sciences, University of Calgary, Calgary, Alberta, Canada T2N 1N4
[b] Department of Mechanical and Manufacturing Engineering, Schulich School of Engineering, University of Calgary, Calgary, AB, Canada
[c] The Canadian Neutron Beam Centre, National Research Council, Chalk River, Ontario, Canada

ARTICLE INFO

Article history:
Received 1 September 2009
Received in revised form 18 December 2009
Accepted 21 December 2009
Available online 28 December 2009

Keywords:
Small multidrug resistance protein (SMR)
Small angle neutron scattering (SANS)
SDS-Tricine PAGE
EmrE
Quaternary ammonium compound (QAC)
Multimerization
Fluorescence

ABSTRACT

Escherichia coli multidrug resistance protein E (EmrE) is a four transmembrane α-helix protein, and a member of the small multidrug resistance protein family that confers resistance to a broad range of quaternary cation compounds (QCC) via proton motive force. The multimeric states of EmrE protein during transport or ligand binding are variable and specific to the conditions of study. To explore EmrE multimerization further, EmrE extracted from *E. coli* membranes was solubilized in anionic detergent, sodium dodecyl sulphate (SDS), at varying protein concentrations. At low concentrations (≤1 μM) in SDS–EmrE is monomeric, but upon increasing EmrE concentration, a variety of multimeric states can be observed by SDS-Tricine polyacrylamide gel electrophoresis (PAGE). Addition of the (QCC), tetraphenyl phosphonium (TPP), to SDS–EmrE samples enhanced EmrE multimer formation using SDS-Tricine PAGE. The relative shapes of EmrE multimers in SDS with or without TPP addition were determined by small angle neutron scattering (SANS) analysis and revealed that EmrE dimers altered in conformation depending on the SDS concentration. SANS analysis also revealed that relative shapes of larger EmrE multimers (≥100 nm sizes) altered in the presence of TPP. Circular dichroism spectropolarimetry displayed no differences in secondary structure under the conditions studied. Fluorescence spectroscopy of SDS–EmrE protein demonstrated that aromatic residues, Trp and Tyr, are more susceptible to SDS concentration than TPP addition, but both residues exhibit enhanced quenching at high ligand concentrations. Hence, EmrE forms various multimers in SDS that are influenced by detergent concentration and TPP substrate addition.

1. Introduction

Ethidium multidrug resistance protein (EmrE) is a member of the small multidrug resistance (SMR) protein family that actively effluxes a broad range of quaternary cation compounds (QCC) by proton motive force [1–3]. SMR protein family members are part of the drug/metabolite transporter (DMT) superfamily which consists of 14 phylogenetically distinct protein families [4,5]. Members of the SMR family are unique from other DMT superfamily members for two important reasons. Firstly, SMR sequences are frequently identified within the conserved regions of Class 1 and 2 integrons (for examples refer to [6,7]) indicating that members of the SMR protein family are highly transmissible via lateral gene transfer. Secondly, SMR proteins are distinct from much larger multidrug transporters (composed of 8 to 22 transmembrane (TM) strands) due to their short length of approximately 100–150 amino acids and form 4 TM α-helix strands within the plasma membrane. These proteins are very hydrophobic and possess a highly conserved negatively charged residue (Glu14 according to *Escherichia coli* EmrE) within the first TM strand that is responsible for its ligand binding activity (as reviewed by [8,9]). *E coli* EmrE serves as the paradigm SMR protein for both functional and structural studies since it is the only member tested extensively biochemically (as reviewed by [9]) and to have yielded high resolution structures by 3-dimensional X-ray crystal diffraction [10] and 3D cryo-electron microscopic analysis of two-dimensional (2D) crystals [11–14]. Despite these achievements, controversy still engulfs EmrE structural elucidation largely due to the difficulties confidently linking EmrE biochemical data to the high resolution structures [15–18].

One of the numerous problems hindering the structural resolution of EmrE is the variability in its arrangement within commonly used membrane mimetics during structural characterization. Studies examining EmrE multimerization in various membrane mimetic environments suggest that the protein is functional in an oligomeric state [19], of which the minimum number of subunits required is a dimer (as reviewed by [8]). EmrE multimers vary in other studies, where multimeric states such as trimers [20,21] and tetramers [12,13]

* Corresponding author. BI 156 Biological Sciences Building, 2500 University Drive N.W., Department of Biological Sciences, University of Calgary, Calgary, Alberta, Canada T2N 1N4. Tel.: +1 403 220 4308; fax: +1 403 289 9311.
E-mail address: turnerr@ucalgary.ca (R.J. Turner).

0005-2736/$ – see front matter © 2009 Elsevier B.V. All rights reserved.
doi:10.1016/j.bbamem.2009.12.017

are also identified using common biochemical and biophysical experiments for membrane protein characterization. One explanation for EmrE multimer variation may be a result of folding alterations caused by the addition of various purification fusion tags to the EmrE protein. Most studies use recombinant SMR proteins possessing FLAG (DYKDDDDK), myc (EQKLISEEDL), hexahistidinyl (His_6) or green fluorescent protein (GFP) tag fusions at their C-terminus for topological determination or for protein purification (as reviewed by [8]).

The objective of this study is to examine the multimerization of untagged EmrE protein solubilized in the simple anionic detergent sodium dodecyl sulphate (SDS). Previous studies of untagged EmrE solubilized in SDS indicated that the protein is monomeric but maintained the ability to bind substrate [22]. Solubilization of most proteins in SDS is generally denaturing; however, biochemical studies of a growing number of integral membrane proteins indicate that membrane proteins are not completely denatured by SDS [23]. Our early work demonstrated that SDS solubilized EmrE has a slightly more open structure (by fluorescence) but similar secondary structure (by circular dichroism) [24]. Hence, further characterization of SDS–EmrE in the presence and absence of a commonly used quaternary cation compound (QCC) substrate, tetraphenyl phosphonium (TPP), was used to explore EmrE conformations in SDS. The ligand TPP is a phase-transfer catalyst commonly used in organic/inorganic synthesis reactions, it is a transportable substrate of EmrE, and has been used as a compound to induce EmrE crystal formation for X-ray diffraction techniques (for example [25]). The studies herein demonstrate that EmrE protein (at low and high concentrations) solubilized in SDS (at 0.2 and 1.0% w/v) promote a diverse range of stable multimers shown by SDS-Tricine polyacrylamide gel electrophoresis (PAGE) and small angle neutron scattering (SANS). Circular dichroism spectroscopy confirmed that the protein was α-helix rich and that secondary structure content was unaffected under the various conditions studied. Additionally, fluorescence spectroscopic experiments of SDS–EmrE were performed to determine any differences in aromatic residue environments within the protein under various conditions studied here with and without TPP. The results from these studies indicate that SDS does not completely denature EmrE protein and that stable multimer forms are present and dependent on protein concentration, which are capable of interacting with TPP ligand.

2. Results

2.1. SDS–EmrE multimerization is dependent upon protein concentration by SDS-Tricine PAGE

In order to examine EmrE multimerization our initial intention was to screen numerous detergents used in previous experiments for their ability to promote EmrE multimers. To begin, the anionic detergent SDS was selected as a simple control system based on previous experiments that showed that SDS promoted a predominately monomeric form of EmrE at low protein concentrations [22,26]. EmrE protein dilutions were prepared, where a starting amount of 1 μg to 10 mg of total protein was dried under N_2 gas and re-suspended into SDS solutions of either 0.2% or 1.0% (w/v). EmrE protein concentrations at or below 0.25 mg/ml (21 μM) in 0.2% SDS (data not shown) and 0.10 mg/ml (8.5 μM) in 1.0% SDS resulted in a predominately monomeric distribution of the protein as determined by SDS-Tricine PAGE (Fig. 1A). Initial re-suspension amounts of EmrE in excess of 0.50 mg protein resulted in SDS–EmrE solutions forming "ladder- like" distributions of EmrE multimers. Based on the corresponding molecular weight of each protein band (as visualized by SDS-Tricine PAGE in kilodaltons (kDa)), EmrE was distributed into monomers (11 kDa), dimers (22 kDa), trimers (33 kDa), hexamers (66 kDa), octamers (88 kDa) and decamers (110 kDa). Although the presence of EmrE multimers is apparent, the most abundant form of the protein resided as a monomer based on the intensity of the EmrE monomer band on the gel. It is important to note that much larger EmrE multimers (>110 kDa) were evident, but accurate molecular weights for these complexes could not be reliably assigned from the gels.

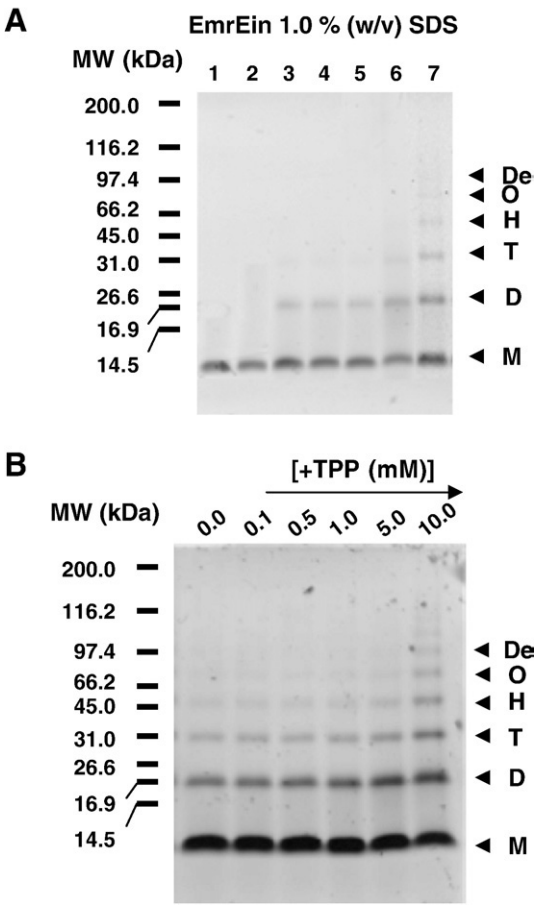

Fig. 1. SDS solubilized EmrE protein multimerization in the absence and presence of TPP ligand. Protein bands were separated by SDS-Tricine PAGE (12%) and visualized by UV absorbance after trichloroethanol (TCE) staining. A total of 3 μg of EmrE protein was loaded into each gel lane in all panels shown. Arrows on the right hand side of each gel image correspond to predicted EmrE multimers based on the estimated molecular weight (MW) of the protein bands in kilodaltons (kDa); monomer (M) 11 kDa, dimer (D) 22 kDa, trimer (T) 33 kDa, hexamer (H) 66 kDa, octamer (O) 88 kDa, and decamer (De) 110 kDa. A) EmrE protein re-suspended into 1.0% (w/v) SDS starting from initial dried EmrE amounts of 0.010 mg (lane 1), 0.025 mg (lane 2), 0.050 mg (lane 3), 0.075 mg (lane 4), 0.100 mg (lane 5), 0.500 mg (lane 6) and 1.000 mg (lane 7) protein. B) Addition of TPP ligand to 1.0% (w/v) SDS-solubilized 21 μM EmrE protein. TPP was added to 1.0% (w/v) SDS–21 μM EmrE samples at final concentrations ranging from 0.1 mM to 10 mM as indicated above each gel lane.

2.2. SDS–EmrE multimer formation and distribution is altered in the presence of TPP

To determine if the multimerization ability of EmrE proteins is altered in the presence of substrate, we examined the effect of increasing TPP addition to SDS–EmrE protein by SDS-Tricine PAGE. Incubation of 0.2% and 1.0% (w/v) SDS solubilized EmrE protein at 8.5 μM (0.10 mg/ml) and 21 μM (0.25 mg/ml) concentrations with 1 mM and 10 mM ligand for 1 h at room temperature produced different amounts of EmrE multimers (Fig. 1B; Table 1). TPP added to either 0.2% or 1.0% SDS–EmrE (8.5 or 21 μM protein) at a final concentration of 1 mM or greater, resulted in an overall increase in all multimer forms with a concomitant decrease in EmrE monomers (Fig. 1B; Table 1). The amount of EmrE multimers induced by 0.2% (w/v) SDS–EmrE protein

Table 1
Summary of EmrE multimer distributions in 0.2% and 1.0% SDS detergent with increasing concentrations of TPP by SDS-Tricine PAGE.

EmrE protein (μM)	TPP (mM)	Mean EmrE protein multimers observed by SDS-Tricine PAGE					
		Decamer (110 kDa)	Octamer (88 kDa)	Hexamer (66 kDa)	Trimer (33 kDa)	Dimer (22 kDa)	Monomer (11 kDa)
0.2% (w/v) SDS							
8.5	–	–	–	–	0.01 ± 0.01	0.16 ± 0.04	0.84 ± 0.09
	1	–	–	–	0.02 ± 0.00	0.25 ± 0.03	0.73 ± 0.08
	10	–	0.05 ± 0.02	0.07 ± 0.03	0.16 ± 0.02	0.34 ± 0.05	0.38 ± 0.08
21	–	–	–	0.02 ± 0.01	0.06 ± 0.02	0.27 ± 0.03	0.65 ± 0.05
	0.1	–	–	0.02 ± 0.01	0.06 ± 0.03	0.27 ± 0.04	0.65 ± 0.08
	0.5	–	–	0.01 ± 0.00	0.06 ± 0.02	0.27 ± 0.03	0.65 ± 0.06
	1	–	–	0.02 ± 0.02	0.06 ± 0.04	0.29 ± 0.05	0.62 ± 0.08
	5	–	0.01 ± 0.00	0.02 ± 0.00	0.09 ± 0.04	0.44 ± 0.05	0.44 ± 0.09
	10	0.02 ± 0.01	0.04 ± 0.03	0.05 ± 0.03	0.16 ± 0.03	0.43 ± 0.12	0.31 ± 0.07
1.0% (w/v) SDS							
8.5	–	–	–	0.02 ± 0.02	0.06 ± 0.06	0.22 ± 0.05	0.69 ± 0.14
	1	–	–	0.02 ± 0.02	0.07 ± 0.06	0.22 ± 0.05	0.69 ± 0.14
	10	0.02 ± 0.02	0.05 ± 0.03	0.07 ± 0.03	0.14 ± 0.03	0.27 ± 0.08	0.44 ± 0.02
21	–	–	–	0.02 ± 0.02	0.04 ± 0.02	0.22 ± 0.03	0.73 ± 0.04
	0.1	–	–	0.01 ± 0.02	0.05 ± 0.04	0.24 ± 0.04	0.68 ± 0.10
	0.5	–	–	0.02 ± 0.01	0.06 ± 0.03	0.24 ± 0.05	0.68 ± 0.10
	1	–	0.01 ± 0.01	0.02 ± 0.00	0.07 ± 0.02	0.24 ± 0.05	0.71 ± 0.06
	5	–	0.03 ± 0.01	0.03 ± 0.02	0.10 ± 0.03	0.30 ± 0.04	0.56 ± 0.08
	10	0.03 ± 0.01	0.06 ± 0.02	0.06 ± 0.02	0.11 ± 0.02	0.29 ± 0.06	0.53 ± 0.05

Protein concentrations: 0.1 mg/ml EmrE = 8.5 μM EmrE, 0.25 mg/ml EmrE = 21 μM EmrE.

was reduced in comparison to those formed in the higher SDS (1.0%) concentration. A possible explanation for the differences in EmrE multimerization under low to high SDS concentrations is due to lower (0.2% w/v; 7 mM) SDS concentrations failing to provide sufficient micelle coverage for the larger protein complexes. In particular, EmrE protein at high concentrations (≥0.1 mg/ml; ≥8.5 μM), despite SDS being above the experimentally determined critical micelle concentration (0.8–1.5 mM in SMR-B buffer). The concentrations of ligand required to visualize the multimer increase on SDS-Tricine PAGE were much higher (≤1 mM TPP) than the previously reported K_D values of 4.8 μM for EmrE in SDS [22]. This indicates that the observed EmrE oligomer stabilization or enhancement requires ligand concentrations far in excess of the K_D to completely saturate all the drug binding sites.

2.3. SANS analysis reveals at least two populations of EmrE multimers in SDS solution

To determine the dimensions of these EmrE multimer complexes present, SANS analysis was used to determine the size of EmrE in SDS detergent. Deuterated SDS (*d*-SDS) was used in place of hydrogenated SDS to enhance the contrast between EmrE within the detergent micelle. If the solvent (water) is contrast-matched (CM) with *d*-SDS, we expect to obtain the scattering pattern of EmrE alone (making *d*-SDS "invisible" due to the differences in deuterium/hydrogen scattering angles). Before experiments were performed using *d*-SDS solubilized EmrE, examination of the contrast-matching conditions of SDS scattering conditions were performed. SANS spectra of 0.2% (w/v) hydrogenated SDS (*h*-SDS) and 0.2% (w/v) *d*-SDS both in SMR-B buffered CM water are shown in Fig. 2A. SDS is known to form spherical micelles [27], which agree with SANS spectrum of 0.2% (w/v) *h*-SDS characterized by a low-q intensity plateau followed by a q^{-4} decay. SANS data of the *d*-SDS solution alone reveals an intensity plateau of q>0.01 Å^{-1} (where SDS micelles become almost "invisible"), indicating a reasonably good CM condition. Therefore, *d*-SDS contrast-matching conditions were achieved and analysis of EmrE protein could be performed.

Fig. 2B–C shows SANS results of 8.5 μM and 21 μM EmrE in 0.2% (w/v) *d*-SDS CM solutions after subtraction of the *d*-SDS CM solution. The SANS data of 0.2% (w/v) *d*-SDS solubilized 8.5 μM EmrE exhibit two scattering intensity decays of q^{-3} as q<0.007 Å^{-1} and q^{-1} as q>0.1 Å^{-1}. The q^{-3} dependence stems into even lower q ranges and represents a fractal surface of large "clusters" (>1000 Å), which are beyond the length scale of our current probing range [28]. The q^{-1} dependence illustrates a characteristic scattering of cylinders, presumably contributed from EmrE multimers. Fortunately, a nearly plateau regime in scattering intensity between 0.05 and 0.1 Å^{-1} was observed in SANS spectra of Fig. 2, allowing us to obtain the dimension of the EmrE subunits by data fitting this result to a cylindrical model [29] (Fig. 2B). The best-fitting radius and length of the cylindrical EmrE multimers were (13 ± 3) Å and (60 ± 20) Å, respectively. Based on the molecular weight and specific volume of EmrE (13,700 g/mol and 0.77 ml/g, respectively) [30], this dimension leads to an average subunit number of 2 (i.e., dimers). The large "clusters" with a fractal surface could originate from either non-SDS-solvated EmrE aggregates or SDS solvated EmrE multimers of larger size. Either morphology for these larger EmrE multimers as interpreted from SANS data is consistent with the results observed by SDS-Tricine PAGE within the high MW region (Fig. 1).

The SANS data of 21 μM EmrE in 0.2% (w/v) *d*-SDS (Fig. 2C) showed a similar scattering pattern to 0.2% *d*-SDS–8.5 μM EmrE, except with a shorter q^{-1} range due to the scattering from the large "clusters" that extend into a higher scattering intensity q range. It should be noted that, although the EmrE concentration was only threefold greater than the 8.5 μM EmrE/*d*-SDS sample, the scattering intensities within the low-q (<0.006 Å^{-1}) region of the spectrum were about tenfold. This difference in scattering intensity indicates that the population ratio of large EmrE "clusters" compared to cylindrical multimers was influenced by EmrE concentration. Although the q^{-1} decay is not as clear as that of the 8.5 μM EmrE sample, fitting these data with the cylindrical model provides us the approximate volume of the protein multimer resulting in a best-fitting radius of (19 ± 3) Å and length of (63 ± 35) Å, where an average EmrE subunit number of ~4 (tetramer) was predicted. The increase in EmrE multimer size (2→4 subunits) in 0.2% *d*-SDS indicated that higher EmrE concentrations promoted larger average EmrE subunit numbers, as observed by SDS-Tricine PAGE analysis (Fig. 1). However, SANS data collected for 0.2% *d*-SDS–EmrE samples with added TPP (1 mM) were nearly identical to those without TPP at each corresponding EmrE concentration (Fig. 2C) revealing that TPP

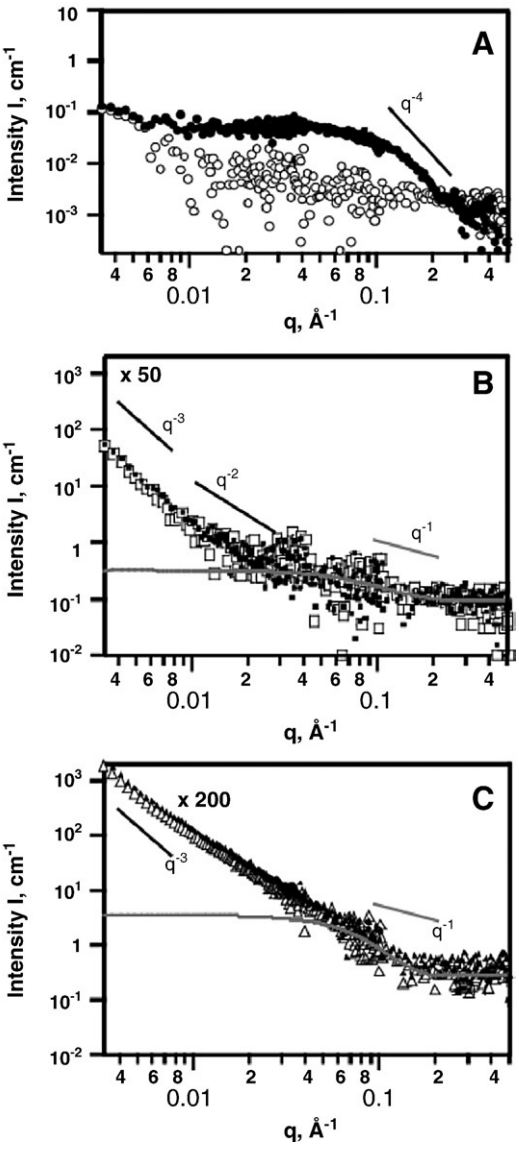

Fig. 2. SANS spectra of 0.2% (w/v) *d*-SDS-solubilized EmrE protein in the presence and absence of TPP. SANS spectra of 0.2% (w/v) *d*-SDS in CM buffer (open circles) and 0.2% (w/v) *h*-SDS in CM buffer (solid circles) baseline solutions for determination of contrast-matching (CM) conditions are shown in panel A. SANS spectra of 0.2% (w/v) *d*-SDS in CM buffer (open circles) and 0.2% (w/v) *h*-SDS in CM buffer (solid circles). Panel B shows SANS spectra collected for 8.5 μM EmrE/0.2% (w/v) *d*-SDS in CM buffer before added ligand (open squares) and after 1 mM TPP addition (solid squares). Panel C shows SANS spectra collected for 21 μM EmrE/0.2% (w/v) *d*-SDS in CM buffer before ligand (open triangles) and after 1 mM TPP addition (solid triangles). The grey curves in each panel indicate the best-fit curve result using a cylindrical model of 8.5 and 21 μM EmrE in SDS solutions without TPP. The SANS data and best-fit results of 8.5 and 21 μM EmrE solutions are re-scaled by 50 and 200, respectively for clarity.

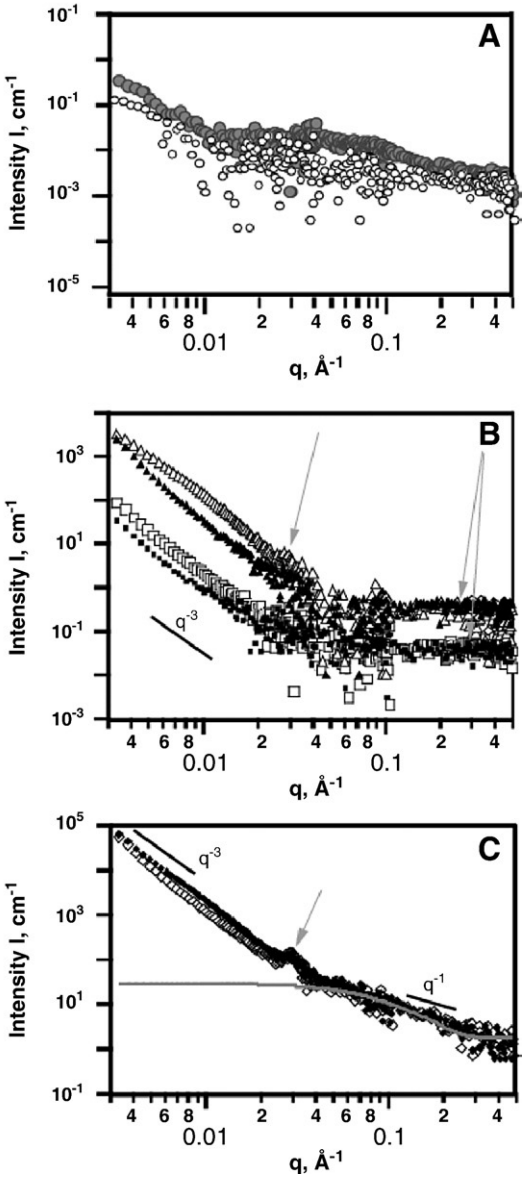

Fig. 3. SANS spectra of 1.0% (w/v) *d*-SDS-solubilized EmrE protein in the presence and absence of TPP. SANS spectra of 0.2% (w/v) *d*-SDS in CM buffer (open circles) and 0.2% (w/v) *h*-SDS in CM buffer (solid circles) baseline solutions for determination of contrast-matching (CM) conditions are shown in panel A. Panel B shows SANS spectra of 1.0% (w/v) *d*-SDS-solubilized EmrE at 8.5 μM (squares) and at 21 μM (triangle) concentrations. Panel C shows SANS spectra of 1.0% (w/v) *d*-SDS-solubilized 64.5 μM EmrE (diamonds). SANS spectra shown in both panels B and C indicate 1.0% (w/v) *d*-SDS-solubilized EmrE before ligand addition (empty symbols) and after 1 mM TPP addition (filled symbol).The grey curve shown in panel C indicate best-fitting curve result of 64.5 μM EmrE using a cylindrical model in SDS solution without TPP. The grey arrows show sharp peaks at $q \sim 0.03$ Å^{-1} (i.e., a regular correlation length ~200 Å) and broad peaks at $q \sim 0.2$ Å^{-1} (i.e., a loose correlation length ~30 Å). The SANS data and best-fit result of 8.5, 21 and 64.5 μM EmrE solutions are re-scaled by 10, 100 and 1000, respectively for clarity.

ligand does not dramatically alter the global morphology of EmrE at low SDS concentrations (0.2% w/v).

SANS data collection of 1.0% (w/v) *d*-SDS in CM solution illustrated a stronger *q*-dependence than that of 0.2% (w/v) *d*-SDS CM solution (Fig. 3A), likely due to the increase in scattering signal from higher micelle content. Applying the same data analysis performed for low *d*-SDS (0.2% w/v) samples, SANS analysis was performed for 8.5 μM, 21 μM and 64.5 μM EmrE in 1.0% (w/v) *d*-SDS (Fig. 3B–C). Due to the increase in *d*-SDS concentration (1.0% w/v), the higher concentration EmrE sample (64.5 μM) could also be determined. SANS spectra of 1.0% *d*-SDS–EmrE samples at 8.5 and 21 μM (Fig. 3B–C) showed differences from the SANS spectra collected for EmrE in 0.2% (w/v) *d*-SDS solutions (Fig. 3B). Although SANS spectra collected at both *d*-SDS concentrations show EmrE scattering intensity (q^{-3}) decay at low-*q* values, no q^{-1} dependence in the high-*q* scattering range was found in 1.0% *d*-SDS–EmrE samples (Fig. 3B). Instead, the high-*q* value data had a plateau region at $q \sim 0.06$ Å^{-1} followed by a seemingly broad peak at $q \sim 0.2$ Å^{-1} (arrows in Fig. 3B–C), indicative of a loose length scale of ~30 Å. This shows the morphology of EmrE multimers likely changed upon the increased concentration of *d*-SDS. Moreover, a sharp peak (with a narrow width of ~0.01 Å^{-1}) was observed at $q \sim 0.03$ Å^{-1} (arrows in Fig. 3B–C), indicating an extremely regular spacing of ~200 Å, for EmrE samples at concentrations of 21 and 64.5 μM. That

this correlation length is independent of EmrE concentration differences indicates a stable, lattice-like structure exists under these high 1.0% (w/v) *d*-SDS conditions. Since this correlation length is not observed for 0.2% (w/v) *d*-SDS–21 μM EmrE samples, it presumably originates from consistently spaced EmrE multimer formation. As for 1.0% *d*-SDS–64.5 μM EmrE, the characteristic of cylindrical scattering pattern observed in SANS spectra of low 0.2% *d*-SDS–EmrE samples was recovered (Fig. 3C). The best-fitting average dimensions of the cylinders were (12 ± 1) Å in radius and (64 ± 15) Å in length. This resulted in an average EmrE subunit number of 1.6 indicating that a high SDS concentration helps solvate EmrE, thus leading to the prediction of a more condensed cylinder.

SANS data collected from EmrE in 1.0% (w/v) *d*-SDS in the presence of 1 mM TPP showed almost identical high-*q* data ($q > 0.05$ Å^{-1}) after comparison to corresponding samples lacking TPP. This indicated no variation of EmrE in local conformations (Fig. 3B–C). Nevertheless, the low-*q* data obtained from SDS–EmrE samples without TPP ligand have lower *q* intensity at EmrE concentrations of 8.5 and 21 μM, unlike the higher *q* intensity of 64.5 μM EmrE samples. These deviations in intensity were presumably due to the variation of population and/or size of the large "clusters" as a result of addition of TPP. However, SANS data of an even lower *q* range will be required to resolve this issue.

2.4. CD spectropolarimetry of SDS–EmrE results in similar levels of α-helix content in the presence or absence of TPP

CD spectropolarimetry was used to monitor any changes in the amount of secondary structure content of the SDS–EmrE preparations under low and high SDS solubilising conditions and in the presence or absence of TPP. CD spectra obtained for 8.5 μM EmrE re-suspended in either 0.2% (w/v) SDS or 1.0% (w/v) SDS were very similar. CD spectrum similarity was confirmed after performing a paired Student's *t*-test that resulted in *P*-values > 0.05 (Fig. 4A). EmrE protein re-suspended in either concentration of SDS resulted in the characteristic CD spectrum for α-helix rich protein (dual λ minima at 208 and 220 nm), where α-helix content estimates ranged from 68 to 73% and from 21 to 26% corresponded to unordered structure after deconvolution. These secondary structure predictions were similar to estimates reported by [24]. The addition of TPP ligand at 0.1 mM and 1 mM final concentration to EmrE in low (0.2%) or high (1.0%) SDS, resulted in CD spectra that were similar to ligand free preparations of SDS–EmrE (Fig. 4B). Estimated α-helix content from the CD spectra of SDS–EmrE in the presence of TPP ligands all resided within the range determined for SDS–EmrE without added ligand after spectrum deconvolution. This suggests that TPP ligand addition does not significantly alter the α-helical content of the EmrE, and that EmrE protein is rich in α-helix content as predicted. The lack of significant secondary structure alteration suggests that TPP interaction with SDS–EmrE likely results in tertiary to quaternary structure alterations only, as shown by SDS-Tricine PAGE and fluorescence of the protein experiments herein.

2.5. TPP quenches EmrE aromatic residues to different extents in SDS by fluorescence spectroscopy

Fluorescence spectroscopy was used to probe for changes in EmrE aromatic amino acid residue environments in the presence and absence of TPP. To accomplish this, we began by determining the intrinsic fluorescence of EmrE in SDS solution to determine conformational differences in low and high concentration SDS environments. EmrE protein possesses sufficient Trp (4 residues) and Tyr (5 residues) residues to be chromophoric. Some of these residues were previously shown to influence both EmrE multimerization (Y40; [31,32]) and its active site (Y4, Y40, and W63; [32–34]). Furthermore, previous fluorescent spectroscopy of EmrE protein and site-directed mutant variants lacking each of the four Trp residues, indicated that its substrate binding was highly influenced by W63 in particular in the presence of ethidium [35]. Hence, the effects of TPP interaction with the protein can be measured by surveying changes in its aromatic residue fluorescent intensity. SDS–EmrE protein fluorescence was monitored at an excitation wavelength of 280 nm to determine the extent of TPP changes to the SDS–EmrE fluorescent spectrum.

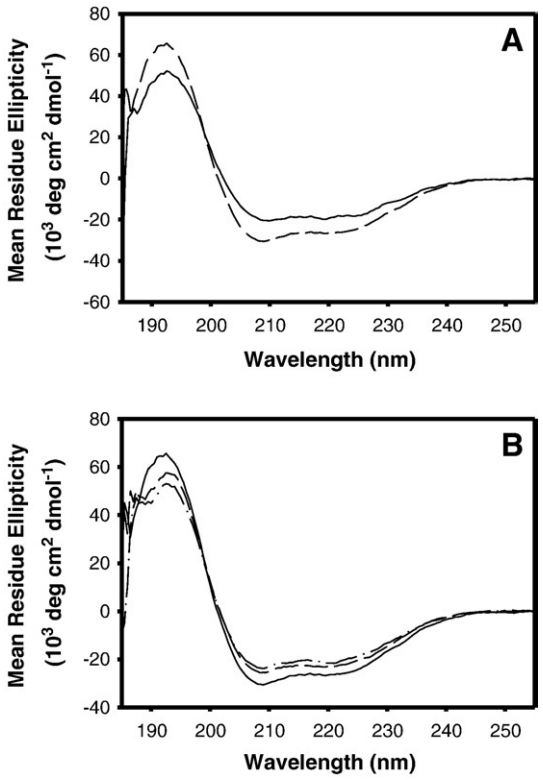

Fig. 4. Far-UV CD spectra of 0.2% (w/v) and 1.0% (w/v) SDS-solubilized EmrE protein in the presence and absence of TPP. Far-UV region (185–255 nm) mean residue ellipticity CD spectra are shown in panel A corresponding to 8.5 μM EmrE protein re-suspended in either 0.2% (w/v) SDS (solid line) or 1.0% (w/v) SDS (dashed line). Panel B shows far-UV mean residue ellipticity CD spectra collected for SDS solubilized 8.5 μM EmrE re-suspended in 0 mM TPP (solid line), 0.1 mM TPP (dashed line) and 1 mM TPP (line–dot–line) respectively.

Emission spectra collected for 0.2% (w/v) SDS solubilized 0.35 μM EmrE lacking added ligand were similar to the spectra for EmrE solubilized at a higher (1.0% w/v) SDS concentration (Fig. 5). However, the degree of Y to W energy transfer was somewhat variable within these preparations, specifically for tyrosine fluorescence contributions, which suggest separation of the transmembrane packing at high detergent concentrations. The trend of fluorescence signal quenching observed for TPP addition to low SDS–EmrE samples resulted in a similar low level of fluorescent quenching (10–25% intensity reduction). Specifically, increasing the concentration of TPP to 0.2% SDS-solubilized EmrE samples resulted in a slight decrease in fluorescence intensity that never exceeded 75% of the total fluorescence signal at the highest concentration of drug surveyed (0.16 mM ligand) (Fig. 5A). Increasing TPP drug concentrations in 0.2% SDS–EmrE did result in a partial to complete loss of Y signal contribution (300–310 nm region) that resulted in a dominant W residue fluorescence signal (Fig. 5A).

Emission spectra obtained for 1.0% (w/v) SDS-solubilized 0.35 μM EmrE demonstrated high contributions of Y fluorescence intensity (λ_{max} ~303–315 nm) in addition to W (shoulder region from 330 to 345 nm) fluorescence within the protein (Fig. 6B). The recurrent dominance of Y emission in 1.0% SDS–EmrE as compared to 0.2% SDS–EmrE, likely results from loss of energy transfer between the Y to W,

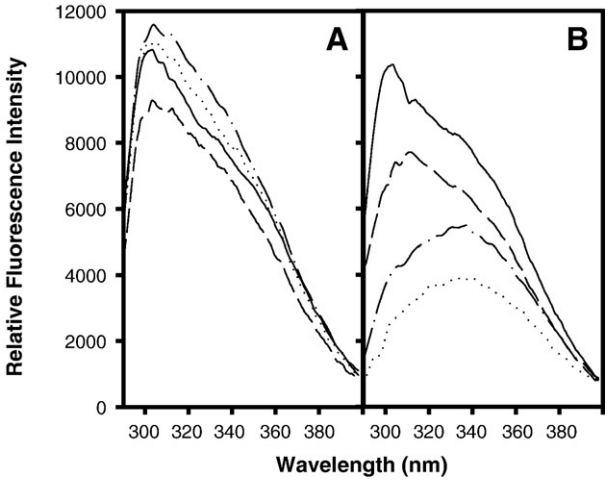

Fig. 5. Fluorescence emission spectra of 0.2% (w/v) and 1.0% (w/v) SDS-solubilized EmrE protein in the presence and absence of TPP. The emission intensity of EmrE samples excited at 280 nm wavelength are shown in arbitrary units and collected within the wavelength region of 290–400 nm. Fluorescent spectra are shown for 0.2% (w/v) solubilized 0.35 μM EmrE samples (panel A) and 1.0% (w/v) solubilized 0.35 μM EmrE (panel B). In both panels TPP was added to both protein sample at final concentrations of 0 mM drug (solid line), 0.016 mM drug (dashed line), 0.081 mM drug (line–dot–line), and 0.16 mM drug (dotted line).

which suggests a more open and dynamic conformation in these regions of the protein. Upon increasing the ligand concentration of TPP (Fig. 5A), the fluorescent intensity and maximum of EmrE showed a gradual loss of Trp intensity (30–45% of the total intensity) (Fig. 5B). TPP at high concentrations resulted in a slight increase in fluorescence intensity by both Y and W residues. The enhanced quenching effect on Trp and Tyr in 1.0% (w/v) SDS–EmrE strongly suggests that higher SDS detergent concentrations enhance the drug binding capability of the protein. As determined by SANS data analysis, the EmrE protein conformation at high SDS differs slightly from those predicted from low SDS–EmrE conformations summarized in Fig. 6.

3. Discussion

Based on the results of these experiments, SDS-solubilized EmrE protein can adopt a diverse range of multimer forms, beginning with primarily monomeric forms at low protein concentrations ranging to increasingly larger multimeric complexes at higher protein concentrations. According to the dimensions estimated from SANS spectra of SDS–EmrE summarized in Fig. 5, we suggest that EmrE dimers form cylinder-like structures in SDS at both low (0.2% w/v) and high (1.0% w/v) concentrations that were tested. It is interesting to note that at low SDS concentrations, the shape of EmrE dimers and tetramers appears to be far less condensed than at higher SDS concentrations studied, suggesting that both the detergent and protein concentration significantly influence TM packing within the protein. The cylinder-like shape of SDS–EmrE dimers contrasts the cube-like conformations of 2D and 3D cryo-EM crystal structures [11–13,36] and X-ray diffracted crystal structure [10] of EmrE, suggesting that SDS influences different TM packing constraints than those detergents used in other studies. High resolution solution-based structural studies involving NMR show that many membrane proteins have flexible or discordant TM segment arrangements in solution than from crystal structures (as reviewed by [37]). Differences such as this may account for cylinder, rather than cube like shapes of EmrE multimer complexes in crystallized EmrE preparations. We recognize that SDS detergent is an unlikely folding environment, in comparison to the plasma membrane, but what is certain is that stable dimer and trimer/tetramer forms of EmrE can be induced in SDS detergent at increasing protein concentrations and yields EmrE oligomer forms observed in other studies of detergent solubilized EmrE [21,33,38].

Moreover, the aromatic residues within EmrE are influenced by the addition of TPP ligand, indicating that the protein does interact with ligand in SDS. The addition of TPP to SDS–EmrE preparations at the detergent concentrations tested does not appear to alter the packing conformation of smaller oligomers, specifically dimers and tetramers as observed in both SANS and SDS-Tricine PAGE analyses (Figs. 1–3). TPP does appear to stabilize the formation of EmrE multimers in SDS, particularly EmrE complexes at or exceeding estimated octamer/hexamer forms. These larger EmrE multimers, observed by SDS-Tricine PAGE at higher MW regions (>96 kDa), are also found in SANS analysis where these larger EmrE complexes likely correspond to the lattice structures (correlation lengths ~200 Å) at the higher SDS concentration (1.0% w/v) examined. EmrE multimer complexes visualized by SDS-Tricine PAGE revealed that higher initial starting amounts of EmrE protein ≥0.5 mg were critical to detect SDS induced EmrE multimers. This corresponds to previous experiments where higher multimers were unobserved in EmrE samples using lower initial starting protein amounts [39] that indicated only monomer forms of EmrE exist in SDS.

EmrE protein adopted numerous multimeric forms in this study, many that were previously observed in experiments involving dodecyl maltoside solubilized tagged EmrE [12,24,39–41]. It is noteworthy that EmrE multimers were also observed in a recent study of Cyan fluorescent protein-tagged EmrE on SDS-PAGE [30], but the presence of EmrE oligomers in these experiments was not discussed. Predicted trimer forms of EmrE were identified from our gels, similar to SDS-PAGE results obtained for C-terminus FLAG tagged *Staphylococcus aureus* homologue of EmrE, Sau-Smr re-suspended in dodecyl maltoside [42]. Our SDS-PAGE experiments showed a noticeable lack of tetramer forms of EmrE according to its estimated MW and instead suggested that EmrE trimer and hexamer forms were present in SDS. However, EmrE tetramers were predicted from the results of our SANS experiments (Fig. 6) and strongly suggest that both EmrE trimer and hexamer forms may correspond to condensed EmrE tetramers and octomeric bundles in these SDS preparations using SDS-PAGE. This is a reasonable assumption as even the monomer form does not migrate exactly to its expected molecular weight. Highly condensed "α-helix bundle-like" forms of EmrE tetramers are predicted for this protein based on other biochemical and *in silico* studies [40,43,44] and would result in a faster electrophoretic mobility of tetramer and octamer forms, consequently reducing its apparent MW in the gel. This phenomenon is often observed in α-helical membrane protein folding studies using SDS-PAGE analysis. In a recent study using various α-helical proteins, changes to the conformation of the protein altered the amount of SDS capable for binding and resulted in 'gel shifting' of these proteins from proposed wild-type conformations [45]. The high proportion of hydrophobic residues within EmrE protein also promote more SDS detergent binding [39] than other integral membrane proteins, thereby altering its electrophoretic mobility in SDS-Tricine PAGE gels as the multimer form increases. As discussed in a recent article focusing on EmrE folding [46] and review [9], this protein is very robust, and can withstand protease cleavage and denaturing environments intolerable for many integral membrane proteins. Therefore, SDS serves as a useful membrane-mimetic system for other studies involving EmrE protein.

Another striking observation from this study was the enhancement of EmrE multimer formation in SDS upon the addition of TPP ligand. SDS-Tricine PAGE results show clear differences in EmrE multimerization, where increasing TPP enhances EmrE multimerization and/or stabilizes existing multimers. This strongly suggests that the drug interaction sites in the SDS–EmrE preparations studied herein are closely linked to regions of the protein involved in EmrE oligomerization. This contrasts DDM solubilization of His-tagged

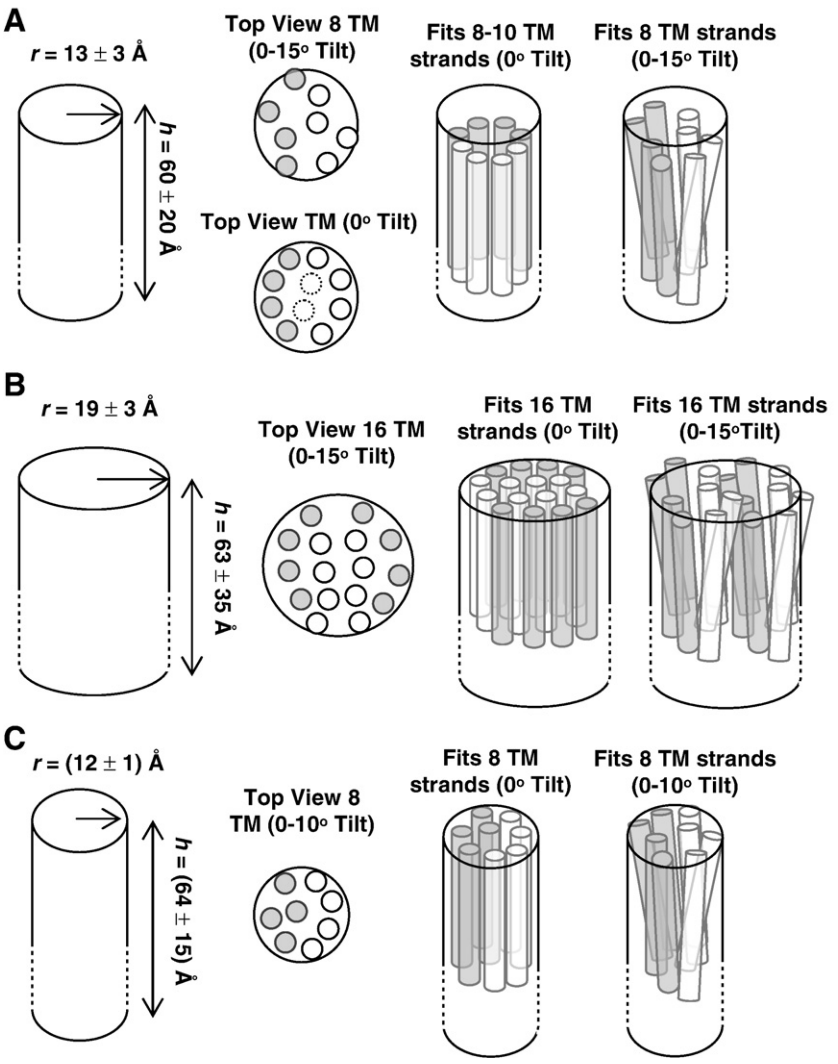

Fig. 6. A cartoon diagram of predicted EmrE dimensions determined from SANS analysis. The estimated dimensions of EmrE protein complexes correspond to large cylinders shown in the far left-hand side of each panel where the radius (r) and height (h) of the cylinder are given above each arrow in angstroms (Å). Thin grey and white cylinders fitted with the larger EmrE cylinder to the right-hand side correspond to individual α-helix TM strands (with dimensions corresponding to a $r = 4.6$ Å and $h = 35$ Å of a 6 turn α-helical TM segment). TM segments were rotated manually at tilt angles of 0°–30° within the indicated r and h of each cylinder shown to the left to determine the degree of TM tilt and approximate number of TM strands each EmrE cylinder could accommodate. Top views shown in each panel are designated as a circle of the same dimensions indicated in the left-hand cylinder and show the number of TM strands that a given complex can accommodate based on TM tilt. Panel A indicates the predicted EmrE complex dimensions for the q^{-1} dependence cylinder of 0.2% (w/v) SDS–8.5 μM EmrE and TM fitting, panel B shows the q^{-1} dependence cylinder of 0.2% (w/v) SDS–21 μM EmrE, and panel C shows the q^{-1} dependence cylinder determined for 1.0% (w/v) *d*-SDS–64.5 μM EmrE.

EmrE which showed that the protein was solely dimeric and that ligand had no effect on protein multimerization [41]. SDS solubilization of membrane proteins has also been shown to promote transition state or intermediate folding states of certain α-helical proteins; the SDS–EmrE conformations studied here may reflect these intermediates necessary for oligomerization unlike DDM where the protein may exist in a non-transitioning state unalterable by ligand interaction.

SANS analysis of SDS–EmrE samples in the presence of TPP also shows variations in the population of the large EmrE "clusters". Fluorescence quenching of SDS–EmrE aromatic residues by TPP appears to reduce the overall Tyr signal intensity under low SDS concentrations, but not the Trp signal. At high SDS concentrations, TPP quenching of both Trp and Tyr are more pronounced. This suggests that TPP interacts with the protein at both SDS concentrations but differences of EmrE conformations such as TM packing may alter the extent of Trp quenching by TPP. Many aromatic residues within SMR proteins are highly conserved (W63, Y4, Y40, and Y60 according to *E. coli* EmrE), and are essential for protein activity regarding both EmrE ligand binding [24,35,47] and multimerization [32,34]. Therefore, the fluorescent quenching trends we observe for TPP confirms that aromatic residues respond to ligand in these SDS–EmrE preparations as in other EmrE experiments involving non-ionic detergents and ligands.

To date, all in depth analyses of EmrE protein structure have been performed in membrane mimetic environments, either in detergents or phospholipids, making it difficult to compare the exact multimeric composition of EmrE *in vivo*. The limitations posed by its short length (110 amino acids) strongly suggest that multimerization is a necessary requirement for its transport activity and has been observed in numerous biochemical and biophysical studies (as reviewed by [8]). However, the precise number of EmrE multimer subunits still remains uncertain within the plasma membrane itself. Based on our studies, we have demonstrated that numerous EmrE oligomers are formed by this protein and stabilized by TPP ligand. This could suggest that EmrE is capable of multimeric flexibility, by altering its subunit amount to correspond to ligands, or that when unconfined in a detergent environment it has more space to accommodate such a large TPP ligand.

4. Conclusion

This study indicates that SDS–EmrE forms multimers in a protein concentration-dependent manner. Thus, EmrE is a robust protein capable of oligomerizing in the anionic detergent SDS. SDS–EmrE multimers appear to be stabilized and enhanced in the presence of its ligand TPP, suggesting that ligands may influence EmrE multimerization.

5. Materials and methods

5.1. Materials used in this study

All chemicals used in this study were purchased from Sigma Aldrich (St Louis, MO, USA) with the following exceptions listed. Organic solvents namely, chloroform, methanol, trichloromethanol and cell growth components tryptone, yeast extract and glycerol were purchased from EMD Chemicals (Darmstadt, Germany). Electrophoresis components such as SDS, tricine, trizma base, acrylamide, and bisacrylamide were obtained from BioRad (Hercules, CA, USA). Deuterated water and deuterated SDS detergent used for SANS experiments were also obtained from Sigma Aldrich.

5.2. Expression and purification of EmrE protein

The plasmid vector pMS119EH [48] encoding the recombinant untagged *E. coli emrE* gene (pEmr-11) was described previously in [26]. EmrE protein accumulation was performed using the transformed *E. coli* cell strain LE392*Δunc* with the pEmr-11 vector grown in 6 l of terrific broth and 100 μg/ml ampicillin to an optical density at 600 nm ($OD_{600\,nm}$) of ~0.5 units. Upon reaching $OD_{600\,nm}$ of 0.5 cells were induced to express the recombinant *emrE* gene with isopropyl thio β-galactoside (IPTG) to a final concentration of 0.1 mM IPTG. Cells were grown for an additional 3 h after induction, harvested by centrifugation at 4000×*g* and stored frozen at −70 °C in SMR-A buffer (50 mM MOPS, 8% glycerol, 5 mM EDTA, 1 mM dithiothreitol (DTT), pH 7). The frozen cell slurry was thawed on ice and phenylmethyl sulphonylfluoride (PMSF) was added to a final concentration of 0.1 mM and French pressed at 800–1000 psi using a Sim-Aminco French Press instrument. Pressed cell slurry was centrifuged at 11,000×*g* for 10 min at 4 °C to remove unbroken cells and subsequently centrifuged in a Beckman-Coulter Optima™ L-90K ultracentrifuge at 40,000 rpm for 90 min at 4 °C in a Ti70 rotor to separate the membrane fraction from the cytosolic fraction. The membrane fraction was re-suspended in SMR-A buffer at a final protein concentration of 10 mg/ml based on modified Lowry Assays [49] and frozen in liquid N_2 for storage at −70 °C.

Frozen membrane preparations were thawed at room temperature (20–25 °C) and subjected to an organic extract procedure in 3:1 chloroform: methanol as described previously [26]. The organically extracted membrane solution was concentrated to 4–10 ml using a Rotovap condenser system. EmrE protein was purified by high pressure liquid chromatography (HPLC) on an AKTA™ Unicorn instrument using an SR10/50 column of LH20 sephadex resin in 1:1 chloroform: methanol solvent. EmrE protein was found to elute within the first peak as monitored by UV absorption at 280 nm ($A_{280\,nm}$). EmrE organic extract fractions were collected together at concentrations ranging from 0.01 mg/ml to 10 mg/ml EmrE protein and dried under N_2 gas in the fume hood for storage at −20 °C.

5.3. SDS detergent re-suspension of EmrE protein and ligand addition

Dried EmrE protein at a variety of initial starting concentrations ranging from 0.001 mg to 15 mg protein was used for these experiments. EmrE protein was re-suspended into 0.2% or 1.0% (w/v) SDS detergent in SMR-B buffer (5 mM MOPS, 10 mM NaCl, 10 μM DTT, pH 7). These solutions were vigorously shaken for 1–2 h to solubilise the protein and then refrozen for 6–14 h at −20 °C. Thawed protein samples were mixed by vortexing for 1 min and sonicated to optical clarity using three, 10 second bursts of 30% sonicating intensity of a Microson XL Ultrasonic cell disrupter. These solutions were centrifuged at 10,000×*g* at room temperature for 10 min to pellet any undissolved material. EmrE protein concentrations were determined by ultraviolet (UV) absorbance spectroscopy with an Ocean Optics UV–visible (Vis)-Spectrophotometer at $A_{280\,nm}$ using the extinction co-efficient (ε) of 29,638 $cm^{-1}\,M^{-1}$.

The QCC ligand used for this study was TPP and was previously shown to bind to the organically extracted EmrE experimentally in SDS, dodecyl maltoside (DDM) and reconstituted vesicles [22]. Additionally, organically extracted EmrE under these conditions was shown to be stable and fold in each membrane mimetic examined [24]. TPP was solubilized in SMR-B buffer to a final concentration of 0.5 M and served as stock solution. TPP was incubated with either 0.2% or 1.0% (w/v) SDS-solubilized EmrE protein at concentrations of 0.1 mg/ml (8.5 μM), 0.25 mg/ml (21 μM), and 0.75 mg/ml (61.5 μM) and incubated at room temperature for a minimum of 1 h. TPP was added to each EmrE protein concentration listed above, ranged from 0.01 mM to 10 mM, depending on the experiment used for study. It should be mentioned that TPP added to SDS solution alone, resulted in the formation of a cloudy precipitate that could not be removed by centrifugation. The precipitate was noted in 0.2% (w/v) SDS solutions with and without solubilized EmrE protein at TPP concentrations at or above 1.0 mM and 1.0% (w/v) SDS with TPP at concentrations ≥5.0 mM ligand. However, the TPP induced precipitate in 1.0% (w/v) SDS was reversible after brief sample stirring in the presence of EmrE protein containing samples only. The final molar ratios of detergent to EmrE protein were 824:1 and 4117:1 calculated based on detergent concentrations of 0.2% (7 mM) and 1.0% (35 mM) SDS to 8.5 μM EmrE protein respectively. The final molar ratios of TPP ligand to EmrE ranged from 4.6 to 1250 (calculated from 0.1 mM to 10.0 mM final TPP concentrations and 8.5 μM and 21 μM EmrE protein).

5.4. SDS-Tricine PAGE analysis of EmrE protein

SDS-Tricine PAGE was selected to screen EmrE multimers to permit molecular weight (MW) determination of the various EmrE multimers in these experiments. Due to the presence of SDS within the gel, this system mirrors a "native" environment for our conditions rather than 'native'-PAGE techniques, which are less reliable for accurate MW estimations due to carryover detergent with the protein complexes and inherent charge differences on the protein in its various conformations. All SDS-solubilized EmrE samples with and without TPP were analyzed using 12% SDS-Tricine PAGE. Trichloroethanol (TCE) was added to the gels during casting, at a final concentration of 0.5% (v/v) TCE, to visualize EmrE tryptophan residues (4 Trp/protein) by UV irradiation at 300 nm according to the method described by Ladner et al. [50]. The TCE staining technique increased the ability to visualize the EmrE protein multimers in the gel by 62% in comparison to conventional coomassie staining, with no difference in migration of the protein. EmrE protein samples were loaded onto the SDS-Tricine PAGE gels to a final amount of 3 μg in the presence or absence of ligand surveyed.

To address the potential issue of SDS removal from the protein by TPP, Tricine SDS-PAGE experiments were performed to solubilize EmrE with greater amounts of SDS to saturate the protein while keeping the same TPP concentrations. To ensure that TPP is the underlying cause of the multimerization at the current (0.2% or 1.0% w/v) SDS concentration, EmrE multimerization was tested at higher SDS concentrations. Supplementary Fig. 1 shows the results from these experiments, and indicates that EmrE multimerization is identical at SDS concentrations of 4.0% (w/v) and 8.0% (w/v) in the presence or absence of TPP (at the same concentrations cited above)

and resulted in multimeric phenomenon similar to lower SDS concentrations used in the original experiments. Experiments were also performed to increase SDS concentrations to either 4.0% and 8.0% (w/v) SDS by adding buffered SDS to ligand pre-incubated 0.2% SDS and 1.0% SDS solubilized EmrE samples and showed no differences in EmrE band intensity. Since no alterations to EmrE multimerization can be observed in either experiment, it is unlikely that TPP is removing SDS from the protein at the detergent concentrations used in this study.

EmrE protein band intensity was normalized by its intensity and molecular weight in kilodaltons (kDa), according to the amount of BioRad low range and polypeptide molecular weight standards to correct for TCE staining differences. Once protein bands were normalized, the overall intensity of each protein band was reported as the percentage of the total amount of protein loaded (3 μg protein). Experiments were repeated a minimum of three times and average EmrE protein band percentage values are reported in Table 1. All protein band intensity measurements were collected from TCE stained SDS-Tricine (12%) PAGE gels using the Kodak 1D™ software package.

5.5. Small angle neutron scattering (SANS) analysis of EmrE protein

Purified EmrE protein was re-suspended into 0.2% or 1.0% (w/v) deuterated SDS (*d*-SDS) in contrast-matched (CM) solvent, whose scattering length density matches with that of the *d*-SDS. The contrast-matched solvent consisted of a mixture of hydrogenated water (*H*) and deuterated water (*D*) with a volume ratio $D/H = 9/1$ that was experimentally determined to minimize the coherent scattering intensity from the *d*-SDS solutions through a series of *D*/*H* compositions. The CM solvent was prepared in SMR-B buffer (5 mM MOPS, 10 mM NaCl, 10 μM DTT, pH 7), such that its total hydrogen content was below 0.05% of the total hydrogen content of the solution, which did not alter contrast-matching conditions. The *d*-SDS re-suspended EmrE protein solutions for SANS experiments were prepared as described in the above sections; EmrE protein concentrations were determined by UV Absorption spectroscopy at $A_{280\,nm}$ ($\varepsilon_{280\,nm}$ 29,638 $cm^{-1}\,M^{-1}$ EmrE). All samples were baseline corrected using their respective *d*-SDS CM SMR-B buffered solution. TPP was prepared to a final concentration of 1 M in CM SMR-B buffered solution and added to each sample at a final concentration of 1 mM.

All SANS experiments were performed at the NG7 30-m Small Angle Neutron Scattering Instrument (NG7 SANS) located at the National Institute of Standards and Technologies (NIST) Centre for Neutron Research (NCNR) in Gaithersburg, Maryland, USA. SANS data are normally reported as the scattered intensity $I(q)$ versus q ($Å^{-1}$), where q represents the scattering vector defined as $\frac{4\pi}{\lambda}\sin(\frac{\theta}{2})$, with λ and θ as the wavelength of neutrons and the scattering angle, respectively. All samples were loaded in standard NCNR demountable cells (with quartz windows) with a sample thickness of 4 mm. The SANS data were collected at a wavelength of 6 Å and three sample-to-detector distances of 1, 5 and 13.2 m to cover a q-range between 0.003 and 0.4 $Å^{-1}$. Raw SANS data were then corrected by the empty cell and background scattering, normalized by the neutron flux and the sample thickness, and put on the absolute scale. Incoherent scattering was determined by the high-q plateau and subtracted from the reduced data.

To determine the shape of EmrE multimers in SDS based on the SANS spectra, SANS data were compared to SANS spectra collected from compounds and polymers of known volume. We identified that a cylindrical model produced the best curve fitting with the lowest RSMD. EmrE transmembrane segments were manually fitted into the predicted cylinders in both 'length-wise' directions shown in Fig. 6 and in the opposite 'width-wise' direction. Width-wise EmrE TM strand fitting into the cylinders poorly accommodated the space requirement posed by the protein to fit all the necessary TM strands since they exceeded the turn angle maximum for the protein. Due to the short connecting loops and turns separating each of the four transmembrane strands based on EmrE secondary structure, limitations to TM tilt angle were considered during TM fitting in both width-wise and length-wise cylinder fits. As a result only the lengthwise fittings are presented herein.

5.6. Circular dichroism spectropolarimetry of EmrE protein

CD spectra were acquired on a JASCO J-810 spectropolarimeter calibrated with (1)-10-camphorsulfonic acid and purged with N_2 at 40–60 l/min. CD spectra of 0.2% and 1.0% SDS-solubilized 8.5 μM EmrE samples used for SDS-Tricine PAGE experiments were measured in the far-UV region (185–260 nm) using 0.10-cm path length quartz cuvettes at room temperature 22 °C, a scan rate of 10 nm/min, a response time of 8 s, and CD spectra were measured in triplicate. CD spectra were corrected by baseline subtraction from their appropriate SDS solution, and were converted to mean residue ellipticity using the molecular weight of EmrE (31,402 g/mol) and 110 amino acid residues. SDS-solubilized EmrE spectra with and without added TPP ligand (0.1 and 1 mM TPP final concentrations) were measured a minimum of three times. Samples containing 1 mM TPP resulted in high amounts scattering below the 200 nm region and required smoothing for subsequent CD spectrum deconvolution. To determine the secondary structure content of EmrE, CD spectrum deconvolution was performed using the Dichroweb package available online [51,52]; deconvolution values from the SELCON and CONTINLL algorithms are cited in the text. The normalized root mean square deviation (NRMSD) values of deconvoluted CD spectra used in this analysis were ≥0.120.

5.7. Fluorescence spectroscopy of EmrE protein

Fluorescence spectroscopic analysis of SDS-solubilized EmrE protein in the presence and absence of TPP was performed using a Fluorolog-Tau-3 Time-resolved spectrofluorometer. Fluorescent spectra were collected in a 1 cm path length quartz cuvette, at an excitation (Ex) wavelength of 280 nm. The emission (Em) spectrum was measured from 290 to 400 nm using double monochrometers for both Ex and Em to reduce scattering artefacts. Both Ex and Em of each sample measured were collected using a 2 nm slit width. All spectra were the average of 6 scans. Fluorescence spectroscopy of SDS-solubilized EmrE protein was performed a minimum of 3 times for each ligand tested.

EmrE protein samples used for fluorescence experiments were selected from SDS-Tricine PAGE experiments and diluted to 0.35 μM EmrE protein from starting concentrations ranging from 21 μM (0.25 mg/ml) EmrE protein samples in either 0.2% and 1.0% (w/v) SDS. TPP ligand was added to SDS–0.35 μM EmrE protein samples at the same mol ratios used for SANS and SDS-Tricine PAGE experiments (12 mol ligand:1 mol EmrE to 588 mol TPP:1 mol EmrE), which corresponded to final QCC concentrations of 0.016 mM, 0.081 mM, and 0.16 mM. A concentration of 0.35 μM EmrE was necessary since higher protein concentrations resulted in increased levels of noise in fluorescence signal intensity when TPP was added.

To address whether the Cl^- counter ion of TPP^+ had any quenching affects on Trp and Tyr quenching within all SDS–EmrE samples, the experiments described were repeated above using the same molar concentrations of NaCl and KBr salts in the place of TPP^+ (Cl^-) ligand. No alteration to the SDS–EmrE fluorescent spectra was observed in these experiments (data not shown).

Acknowledgements

We would like to thank S. Sarro, B. Lyle, and T. Winstone for their technical assistance during protein purification and Dr. S. Kline (NIST

Centre for Neutron Research; Gaithersburg, Maryland, USA) for SANS assistance. This work was funded by a National Science and Engineering Research Council (NSERC) operating grant to RJT and utilized facilities supported in part by the National Science Foundation (USA) under Agreement No. DMR-0454672.

Appendix A. Supplementary data

Supplementary data associated with this article can be found, in the online version, at doi:10.1016/j.bbamem.2009.12.017.

References

[1] L. Grinius, G. Dreguniene, E.B. Goldberg, C.H. Liao, S.J. Projan, A staphylococcal multidrug resistance gene product is a member of a new protein family, Plasmid 27 (1992) 119–129.
[2] T.G. Littlejohn, I.T. Paulsen, M.T. Gillespie, J.M. Tennent, M. Midgley, I.G. Jones, A.S. Purewal, R.A. Skurray, Substrate specificity and energetics of antiseptic and disinfectant resistance in *Staphylococcus aureus*, FEMS Microbiol. Lett. 74 (1992) 259–265.
[3] H. Yerushalmi, M. Lebendiker, S. Schuldiner, EmrE, an *Escherichia coli* 12-kDa multidrug transporter, exchanges toxic cations and H+ and is soluble in organic solvents, J. Biol. Chem. 270 (1995) 6856–6863.
[4] D.L. Jack, N.M. Yang, M.H. Saier Jr., The drug/metabolite transporter superfamily, Eur. J. Biochem. 268 (2001) 3620–3639.
[5] M.H. Saier Jr., I.T. Paulsen, Phylogeny of multidrug transporters, Semin. Cell Dev. Biol. 12 (2001) 205–213.
[6] S.J. Rosser, H.K. Young, Identification and characterization of class 1 integrons in bacteria from an aquatic environment, J. Antimicrob. Chemother. 44 (1999) 11–18.
[7] I. Rodriguez, M.C. Martin, M.C. Mendoza, M.R. Rodicio, Class 1 and class 2 integrons in non-prevalent serovars of *Salmonella enterica*: structure and association with transposons and plasmids, J. Antimicrob. Chemother. 58 (2006) 1124–1132.
[8] D.C. Bay, K.L. Rommens, R.J. Turner, Small multidrug resistance proteins: a multidrug transporter family that continues to grow, Biochim. Biophys. Acta 1778 (2008) 1814–1838.
[9] S. Schuldiner, EmrE, a model for studying evolution and mechanism of ion coupled transporters, Biochim. Biophys. Acta 1794 (2009) 748–762.
[10] Y.J. Chen, O. Pornillos, S. Lieu, C. Ma, A.P. Chen, G. Chang, X-ray structure of EmrE supports dual topology model, Proc. Natl. Acad. Sci. U. S. A. 104 (2007) 18999–19004.
[11] C.G. Tate, E.R. Kunji, M. Lebendiker, S. Schuldiner, The projection structure of EmrE, a proton-linked multidrug transporter from *Escherichia coli*, at 7 A resolution, Embo J. 20 (2001) 77–81.
[12] C.G. Tate, I. Ubarretxena-Belandia, J.M. Baldwin, Conformational changes in the multidrug transporter EmrE associated with substrate binding, J. Mol. Biol. 332 (2003) 229–242.
[13] I. Ubarretxena-Belandia, J.M. Baldwin, S. Schuldiner, C.G. Tate, Three-dimensional structure of the bacterial multidrug transporter EmrE shows it is an asymmetric homodimer, Embo J. 22 (2003) 6175–6181.
[14] C.G. Tate, Comparison of three structures of the multidrug transporter EmrE, Curr. Opin. Struct. Biol. 16 (2006) 457–464.
[15] S. Schuldiner, Controversy over EmrE structure, Science 317 (2007) 748–751 author reply 748–51.
[16] S. Schuldiner, When biochemistry meets structural biology: the cautionary tale of EmrE, Trends Biochem. Sci. 32 (2007) 252–258.
[17] C. Miller, Pretty structures, but what about the data? Science 315 (2007) 459.
[18] V.M. Korkhov, C.G. Tate, An emerging consensus for the structure of EmrE, Acta Crystallogr. D Biol. Crystallogr. 65 (2009) 186–192.
[19] D. Rotem, N. Sal-man, S. Schuldiner, *In vitro* monomer swapping in EmrE, a multidrug transporter from *Escherichia coli*, reveals that the oligomer is the functional unit, J. Biol. Chem. 276 (2001) 48243–48249.
[20] H. Yerushalmi, S. Schuldiner, An essential glutamyl residue in EmrE, a multidrug antiporter from *Escherichia coli*, J. Biol. Chem. 275 (2000) 5264–5269.
[21] T.R. Muth, S. Schuldiner, A membrane-embedded glutamate is required for ligand binding to the multidrug transporter EmrE, Embo J. 19 (2000) 234–240.
[22] C.W. Sikora, R.J. Turner, Investigation of ligand binding to the multidrug resistance protein EmrE by isothermal titration calorimetry, Biophys. J. 88 (2005) 475–482.
[23] J. Song, M.S. Lee, I. Carlberg, A.V. Vener, J.L. Markley, Micelle-induced folding of spinach thylakoid soluble phosphoprotein of 9 kDa and its functional implications, Biochemistry 45 (2006) 15633–15643.
[24] S.L. Federkeil, T.L. Winstone, G. Jickling, R.J. Turner, Examination of EmrE conformational differences in various membrane mimetic environments, Biochem. Cell Biol. 81 (2003) 61–70.
[25] V.M. Korkhov, C.G. Tate, Electron crystallography reveals plasticity within the drug binding site of the small multidrug transporter EmrE, J. Mol. Biol. 377 (2008) 1094–1103.
[26] T.L. Winstone, K.A. Duncalf, R.J. Turner, Optimization of expression and the purification by organic extraction of the integral membrane protein EmrE, Protein Expr. Purif. 26 (2002) 111–121.
[27] J.B. Hayter, J. Penfold, Self-consistent structural and dynamic study of concentrated micelles solutions, J. Chem. Soc., Faraday Trans. 1 (77) (1981) 1851–1863.
[28] J.S. Higgins, H.C. Benoît, Polymers and Neutron Scattering, Oxford University Press Inc., NY, USA, 1994.
[29] S.R. Kline, Reduction and analysis of SANS and USANS data using IGOR Pro, J. Appl. Crystallogr. 39 (2006) 895–900.
[30] H.S. McHaourab, S. Mishra, H.A. Koteiche, S.H. Amadi, Role of sequence bias in the topology of the multidrug transporter EmrE, Biochemistry 47 (2008) 7980–7982.
[31] S.S. Mordoch, D. Granot, M. Lebendiker, S. Schuldiner, Scanning cysteine accessibility of EmrE, an H+-coupled multidrug transporter from *Escherichia coli*, reveals a hydrophobic pathway for solutes, J. Biol. Chem. 274 (1999) 19480–19486.
[32] M. Sharoni, S. Steiner-Mordoch, S. Schuldiner, Exploring the binding domain of EmrE, the smallest multidrug transporter, J. Biol. Chem. 280 (2005) 32849–32855.
[33] Y. Elbaz, S. Steiner-Mordoch, T. Danieli, S. Schuldiner, In vitro synthesis of fully functional EmrE, a multidrug transporter, and study of its oligomeric state, Proc. Natl. Acad. Sci. U. S. A. 101 (2004) 1519–1524.
[34] D. Rotem, S. Steiner-Mordoch, S. Schuldiner, Identification of tyrosine residues critical for the function of an ion-coupled multidrug transporter, J. Biol. Chem. 281 (2006) 18715–18722.
[35] Y. Elbaz, N. Tayer, E. Steinfels, S. Steiner-Mordoch, S. Schuldiner, Substrate-induced tryptophan fluorescence changes in EmrE, the smallest ion-coupled multidrug transporter, Biochemistry 44 (2005) 7369–7377.
[36] I. Ubarretxena-Belandia, C.G. Tate, New insights into the structure and oligomeric state of the bacterial multidrug transporter EmrE: an unusual asymmetric homodimer, FEBS Lett. 564 (2004) 234–238.
[37] J.K. Rainey, L. Fliegel, B.D. Sykes, Strategies for dealing with conformational sampling in structural calculations of flexible or kinked transmembrane peptides, Biochem. Cell Biol. 84 (2006) 918–929.
[38] H. Yerushalmi, M. Lebendiker, S. Schuldiner, Negative dominance studies demonstrate the oligomeric structure of EmrE, a multidrug antiporter from *Escherichia coli*, J. Biol. Chem. 271 (1996) 31044–31048.
[39] T.L. Winstone, M. Jidenko, M. le Maire, C. Ebel, K.A. Duncalf, R.J. Turner, Organic solvent extracted EmrE solubilized in dodecyl maltoside is monomeric and binds drug ligand, Biochem. Biophys. Res. Commun. 327 (2005) 437–445.
[40] J. Venkatraman, G.A. Nagana Gowda, P. Balaram, Structural analysis of synthetic peptide fragments from EmrE, a multidrug resistance protein, in a membrane-mimetic environment, Biochemistry 41 (2002) 6631–6639.
[41] P.J. Butler, I. Ubarretxena-Belandia, T. Warne, C.G. Tate, The *Escherichia coli* multidrug transporter EmrE is a dimer in the detergent-solubilised state, J. Mol. Biol. 340 (2004) 797–808.
[42] L.L. Grinius, E.B. Goldberg, Bacterial multidrug resistance is due to a single membrane protein which functions as a drug pump, J. Biol. Chem. 269 (1994) 29998–30004.
[43] J. Torres, I.T. Arkin, Recursive use of evolutionary conservation data in molecular modeling of membrane proteins A model of the multidrug H+ antiporter EmrE, Eur. J. Biochem. 267 (2000) 3422–3431.
[44] I.T. Arkin, W.P. Russ, M. Lebendiker, S. Schuldiner, Determining the secondary structure and orientation of EmrE, a multi-drug transporter, indicates a transmembrane four-helix bundle, Biochemistry 35 (1996) 7233–7238.
[45] A. Rath, M. Glibowicka, V.G. Nadeau, G. Chen, C.M. Deber, Detergent binding explains anomalous SDS-PAGE migration of membrane proteins, Proc. Natl. Acad. Sci. U. S. A. 106 (2009) 1760–1765.
[46] D. Miller, K. Charalambous, D. Rotem, S. Schuldiner, P. Curnow, P.J. Booth, *In vitro* unfolding and refolding of the small multidrug transporter EmrE, J. Mol. Biol. 393 (2009) 815–832.
[47] Y. Adam, N. Tayer, D. Rotem, G. Schreiber, S. Schuldiner, The fast release of sticky protons: kinetics of substrate binding and proton release in a multidrug transporter, Proc. Natl. Acad. Sci. U. S. A. 104 (2007) 17989–17994.
[48] J.P. Furste, W. Pansegrau, R. Frank, H. Blocker, P. Scholz, M. Bagdasarian, E. Lanka, Molecular cloning of the plasmid RP4 primase region in a multi-host-range tacP expression vector, Gene 48 (1986) 119–131.
[49] C.M. Stoscheck, Quantitation of protein, Methods Enzymol. 182 (1990) 50–68.
[50] C.L. Ladner, J. Yang, R.J. Turner, R.A. Edwards, Visible fluorescent detection of proteins in polyacrylamide gels without staining, Anal. Biochem. 326 (2004) 13–20.
[51] A. Lobley, L. Whitmore, B.A. Wallace, DICHROWEB: an interactive website for the analysis of protein secondary structure from circular dichroism spectra, Bioinformatics 18 (2002) 211–212.
[52] L. Whitmore, B.A. Wallace, DICHROWEB, an online server for protein secondary structure analyses from circular dichroism spectroscopic data, Nucleic Acids Res. 32 (2004) W668–W673.